The Use of High-Pass Filters and the Inpainting Method to Clouds Removal and Their Impact on Satellite Images Classification

Ana Carolina Siravenha, Danilo Sousa, Aline Bispo, and Evaldo Pelaes*

Signal Processing Laboratory, Federal University of Para (UFPA), Belem, PA, Brazil
{siravenha,danilofrazao,pelaes}@ufpa.br, aline.bispo@itec.ufpa.br

Abstract. This paper proposes a new technique to smooth undesirable elements of the atmosphere, such as fogs, clouds and shadows, which damage and lead to loss of image data. In our approach, an efficient way to detect clouds and shadows is presented. The method applies constants related to such undesirable elements, as well as a High boost Filter in the homomorphic filtering for scattered clouds removal. We highlight the use of the Inpainting method, which replaces contaminated pixels using a nearest neighbor interpolation. Beside this, the proposed algorithm adopts a morphologic opening of the image that aims to suppress some isolated occurrences in the scene. The results are evaluated by Kappa coefficient and PSNR index, proving the good performance of the method.

Keywords: Cloud removal, High boost filtering, cloud detection, inpainting.

1 Introduction

One of the main problems related to remote sensing of images, whether aerial or satellite, is the presence of undesirable elements in the atmosphere such as fog, mist, clouds and the shadows from them. Since the sensing becomes a constant target of these atmospheric components, which commonly occurs in tropical areas, activities such as environmental or urban monitoring, or any other study for extraction of relevant information to users, become impaired.

Due to these problems, various techniques have been developed for the removal or, at least, the mitigation of these effects, especially the clouds, which are more frequent in this type of image. According to the literature, the nature of these techniques depends on the kind of cloud, dense or sparse. The removal of dense clouds and their shadows are basically divided into two approaches, the first relates to the use of a non-cloud cover reference image in a multi-temporal analysis [18], or even doing an interpolation with contribution of a radar image (SAR) [8]. The other approach attempts to estimate what is being covered

* This work was supported by *Fundação de Amparo à Pesquisa do Estado do Pará* and Federal University of Para.

G. Maino and G.L. Foresti (Eds.): ICIAP 2011, Part II, LNCS 6979, pp. 333–342, 2011.

by cloud and/or shadow in image, using the same or similar approaches to the inpainting method [2,12,14].

On the other hand, when it comes to the removal of scattered clouds, the most used method is the homomorphic filtering [3,16,13]. In [7], an evaluation was made among five High-pass filters (HPF), highlighting one that gives the best results, the Butterworth filter.

This paper proposes a technique for removing the elements of the atmosphere that damage and lead to loss of image data. Our method detects clouds and shadows with the aid of constants related to such elements, as well as a High-Boost Filter (HBF) [10,17] to the filtering of scattered clouds. In a comparison with the approach applied in [7], the proposed method was found to be more efficient. The HBF does not totally eliminate the low frequency components of the image, thereby causing smaller information losses. Another important feature of this approach is the use of inpainting method, generally employed for the removal of large objects in an image [1,2]. In this paper, the impainting method is applied for the redefinition of dense blocks of clouds and shadows. By executing a nearest neighbor interpolation [9,6] and using only the information of image pixels to be processed, this method is made more versatile and adaptive to the context. At last, a morphological operation of opening of the image is also applied in this proposed method.

The paper is divided as follows. Section 2 describes the theory of all techniques used in this work as well as how the algorithm works; section 3 shows the results after the application of the algorithms and the evaluation of the methods; and finally, section 4 shows the conclusions about the described method.

2 Methodology

In this section we present the basic techniques employed to develop our cloud and shadow removal algorithm. Each technique is presented and its contribution to the proposed method are described.

2.1 Cloud and Shadow Detection

The basis of the shadows and clouds detection is based on [7], in which is made a separation of regions with different characteristics in the image, in order to improve results. This division is made considering statistical measures of the image, detecting dense and scattered clouds areas.

The presence of clouds in a remote sensing image is usually associated with the presence of shadows. The Sun angle at the scene capture and/or the scene capture in an off-nadir angle[1] are some explanation for the shadows formation in remote sensory images. For this purpose, it was added to the cloud detection algorithm, the shadows detection capability.

[1] The term *off-Nadir* refers to non-orthogonal imaging between the sensor and the imaged object.

The difference on the lighting conditions, on the sensor characteristics and on the surface, make that the images have different ranges of gray levels representing a class. For example, under opposite lighting conditions a same region can be easily labeled as dense and non dense vegetation, or a dense vegetation region can be mislabeled as a shadow region. In order to improve the technique described in [7], making the regions separation more flexible, we added two constants to the detection algorithm, called *cc* and *sc*, cloud and shade constants, respectively. Both constants have default value equals to 1, and after the tests, was noted that the range from 0 to 3 returns optimized results. Therefore, by the change of these values we can differentiate more precisely the classes of a scene.

The process of regions separation is expressed by

$$f(x,y) = \begin{cases} i(x,y) < (sc \times i_{m-dp}), & i(x,y)\epsilon\ 0; \\ (sc \times i_{m-dp}) < i(x,y) < i_m, & i(x,y)\epsilon\ 1; \\ i_m < i(x,y) < (cc \times i_{m+dp}), & i(x,y)\epsilon\ 2; \\ i(x,y) > (cc \times i_{m+dp}), & i(x,y)\epsilon\ 3. \end{cases} \tag{1}$$

where $i(x,y)$ is equal to the pixel value of the noise image (cloud or shadow), i_m represents the average value of the noisy image, $i_{m+dp} = i_m + \sigma_i$ and $i_{m-dp} = i_m - \sigma_i$. Thus, regions defined as 0 are the shadow regions of the image, those defined as 1 are free from any kind of noise, while the regions defined as 2 are labeled as containing scattered clouds and finally those defined as 3 are detected as dense clouds.

2.2 Image Opening

The morphological filters refer to the study of geometric structure of the entities present in an image. Being the filters of dilation and erosion basic morphological operations and based on set theory, this technique involves the interaction between an image A (the object of interest) and a structuring element B. In general, most of the morphological operations are based on simple operations of expansion and shrinkage [5].

Opening generally smooths the contours of an image, breaking narrow isthmus and eliminating thin protrusions, and is defined as follows: the opening of A by B is given by the erosion of A by B, followed by dilation by B, that is, $A \circ B = (A \ominus B) \oplus B$.

Therefore, after opening the image, small objects inside a larger tend to be extinct. Our interest in applying such a morphological transformation, relies on the fact of small objects contained in large blocks defined as noise can worsen the interpolation phase, during the inpainting method. Given this, the opening operation can eliminate this problem, generating a better redefinition of image pixels damaged by atmospheric action.

2.3 Homomorphic Filter

The images usually consist of light reflected from objects. The basic nature of an image can be characterized by two components: (1) the amount of light coming

from the incident source on the scene and (2) the amount of reflected light by objects in the scene. These bands of light are called components of *illumination* and *reflection*, and are denoted by $l(x, y)$ and $r(x, y)$, respectively. The functions l and r combine multiplicatively to produce the F image:

$$F(x, y) = l(x, y)r(x, y), \tag{2}$$

where $0 < l(x, y) < \infty$ e $0 < r(x, y) < 1$.

The Fourier transform of the product of two functions is not separable [7] and it is desirable to manipulate the image in frequency domain, then we apply the natural logarithm function that approximates the function $F(x, y)$ to the form of a sum of the components l and r

$$z(x, y) = \ln F(x, y) = \ln l(x, y) + \ln r(x, y). \tag{3}$$

In frequency domain, we can manipulate the image in terms of low and high components, or illumination and reflection, separately. Then, we apply a Fast Fourier Transform on $z(x, y)$, the natural logarithm of $F(x, y)$

$$\mathscr{F}(z(x, y)) = \mathscr{F}(\ln F(x, y)) = \mathscr{F}(\ln l(x, y)) + \mathscr{F}(\ln r(x, y)). \tag{4}$$

Therefore, considering that Z, L and R are Fourier Transforms of z, $\ln l$ and $\ln r$, respectively, then

$$Z(w, v) = L(w, v) + R(w, v). \tag{5}$$

The advantage of the use of high pass High-boost filter to the cloud removal applications is that it does not completely suppress the lower frequencies. Thus, the filter $H(.)$ is applied to the function Z and assumes

$$S(w, v) = H(w, v)Z(w, v) = H(w, v)L(w, v) + H(w, v)R(w, v) \tag{6}$$

We can take the inverse Fourier transform of Eq. 6

$$s(x, y) = \mathscr{F}^{-1}(H(w, v)L(w, v)) + \mathscr{F}^{-1}(H(w, v)R(w, v)), \tag{7}$$

and finally, as z was obtained using the logarithm of the original image F, the reverse process produces the desired image $\hat{F}$

$$\hat{F} = \exp s(x, y) = \exp\left(l'(x, y)\right) \exp\left(r'(x, y)\right) = l_0(x, y)r_0(x, y). \tag{8}$$

By applying a multiplicative factor of amplification (A) before subtraction of the low frequencies (LPF), we obtain a filter HPF High boost. Thus,

$$\begin{aligned} Highboost &= (A)(original) - LPF \\ Highboost &= (A - 1)(Original) + HPF \end{aligned} \tag{9}$$

where $HPF = Original - LPF$. If $A = 1$, we have a simple filter high-pass. When $A > 1$, a part of the original image is maintained in the output. A Butterworth HPF used in the formulation of this proposed High boost filtering.

Homomorphic filtering using High boost is applied only in the areas labeled as 2, i.e., areas where there is presence of scattered clouds, mists and fogs. The filtering in these regions is suitable, because the region of cloud is a low frequency region due to the homogeneity of its pixels.

Thus, the homomorphic filtering process can be summarized by the Fig. 1.

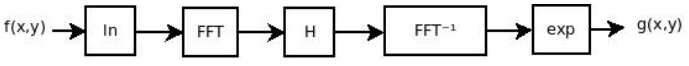

Fig. 1. Homomorphic Filter Schema [3,16]

2.4 Inpainting

Areas labeled as 3 during the separation of regions (Subsection 2.1) are the thickest clouds present in the images, which suffer very little or even no effect of homomorphic filtering. The treatment of these areas is done by a method called inpainting. This method aims to remove large objects, fill gaps, undefined or damaged regions of an image, in order to restore or make it more visible [2,12]. In this paper, we consider as damaged regions to be treated, areas of dense clouds, as done in [14], and shadow regions.

The Inpainting method uses the technique of nearest neighbor interpolation and the effect created is that the nearest pixel appears larger, because its value is assigned to an undefined pixel [9].

Taking a point x to be interpolated and various points x_k neighbors to such, which belong to a set of values of samples of image pixels f_k, a calculation of Euclidean distance is made between this value to be estimated and the neighboring sample values, according to the following equation: $||x - x_k||$. The value of x_k which yields the lowest result in the last equation, has its intensity value assigned to the pixel x, and so continues until all undefined pixels are filled [6].

2.5 Algorithm of the Proposed Method

The steps of the proposed algorithm are shown in sequence:

1. The regions of the image F are mapped as described in Subsection 2.1. The result of this step is an mapped image among the four categories described, called FM.
2. The FM mapped image passes through an opening operation, generating a new image FMO, which will be the base for mapping in the fusions.
3. The *pixels* of image areas F labeled as 0 and 3 are treated as undefined, then the *inpainting* method (Subsection 2.4) assigns new values to these pixels, generating an interpolated image FI.
4. The images F and FI are joined to form the fused image FF. This fusion is done by the combination of the areas 0 and 3 of the FI image, with areas 1 and 2 of the image F.

5. The original image F is passed through homomorphic filter (according Subsection 2.3), removing scattered clouds, and producing an image called FH.
6. The last fusion of images to form the resulting image (FR) is made between images FF and FH. From image FH are extracted the pixels previously classified as type 2, and the remaining pixels are got from the image FF.

The flowchart of the process described above is shown in the diagram of Fig. 2:

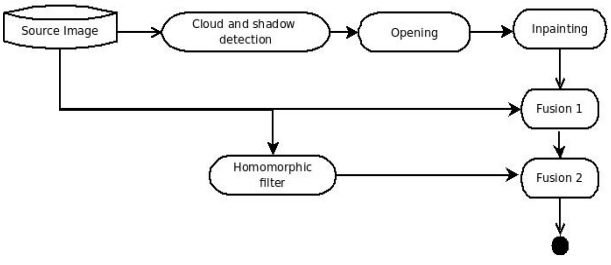

Fig. 2. Flowchart of the proposed algorithm

3 Results and Discussions

In order to exemplify the procedure described previously, we take as *Original image*, we have a scene of city of Rome (Italy), captured by the WORLDVIEW-2 satellite sensor, in 2009. The scene is contaminated with three types of atmospheric damage mentioned in this paper: scattered clouds, dense clouds and shadows (4% of total scene area).

The steps to remove these elements will be evaluated according to the Kappa coefficient of the image [7] and the peak signal to noise ratio (PSNR) index [15,4], based on similarity and compatibility of information between the original and reference images, where bigger values represent the best index achievable. We use two reference images for such evaluations, which passed by a process of manual removal of atmospheric noise simulating optimal pictures, one free of scattered clouds and other free of all kind of noise.

Firstly, the Butterworth filter used by [7] was tested in comparison with High boost approach. In order to remove scattered cloud, the original image was submitted to both filters and compared with a reference image free of scattered clouds. According the metrics cited before, the homomorphic filtering using High boost presented highest accuracy, with $Kappa = 0.7788$ and $PSNR = 21.63dB$, whilst the HPF Butterworth approach presented $Kappa = 0.3973$ and $PSNR = 19.82dB$, showed in Fig. 3. Rather than many HPF, the filter High boost does not totally eliminate the low frequency components, allowing them to assist in image interpretation. Thus, it becomes clear that the High boost filter is more efficient, producing visibly clearer results with less loss of information.

Aiming to remove dense clouds and shadows, still without the constant of regions detection, the inpainting method was applied to both high pass filtering

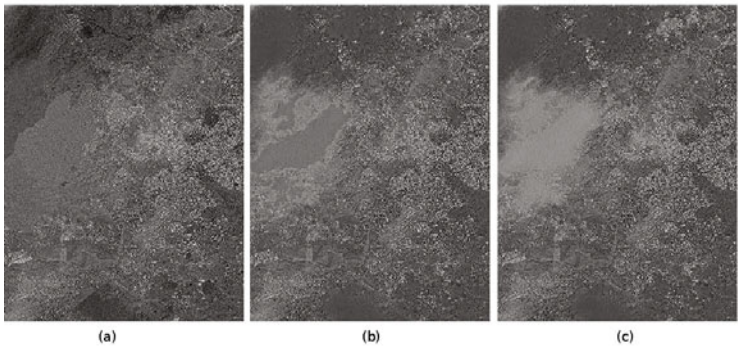

Fig. 3. First test: (a) Original image and scattered clouds removal results using HPF (b) Butterworth ($Kappa = 0.3973$ and $PSNR = +19.82dB$) and (c) High boost ($Kappa = 0.7788$ and $PSNR = +21.63dB$)

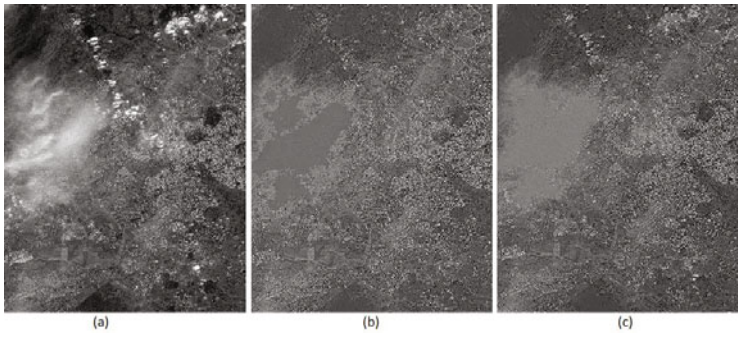

Fig. 4. Second test: (a)Original image and dense clouds and shadows removal results using HPF (b) Butterworth ($Kappa = 0.4618$ and $PSNR = +19.4dB$) and (c) High boost ($Kappa = 0.4737$ and $PSNR = +19.6dB$)

resultant images. To obtain the Kappa coefficient and PSNR indexes were used a manually produced free of noise image. Once more, the approach using High boost got better results, with $Kappa = 0.4737$ and $PSNR = 19.6dB$, over Butterworth approach, with $Kappa = 0.4618$ and $PSNR = 19.4dB$, showed in Fig. 4. Note that the approach that uses the HPF High boost, is slightly more efficient, even with the great similarity between the results. It is also visible the disappearance or smoothing of most noisy regions of the image, despite the decrease in Kappa and PSNR index values, since we have now a high degree of redefinition of pixels, due to the amount of dense clouds and shadows in original image.

Finally, by entering the constants *cn* and *cs*, for the detection of clouds and shadow, respectively, was compared the effect of this insertion in the same scene presented before. Once again, the Butterworth approach presented lower performance than High boost. The Butterworth indexes achieved were $Kappa = 0.5279$

and $PSNR = 19.64dB$, while the High boost indexes achieved were $Kappa = 0.5329$ and $PSNR = 19.94dB$. Therefore, besides the High boost filter remain slightly better than the Butterworth, we see a considerable improvement in efficiency of the method using both filters after use of constants(setted to $cn = 1.3$ and $cs = 0.8$). The results are showed Fig. 5.

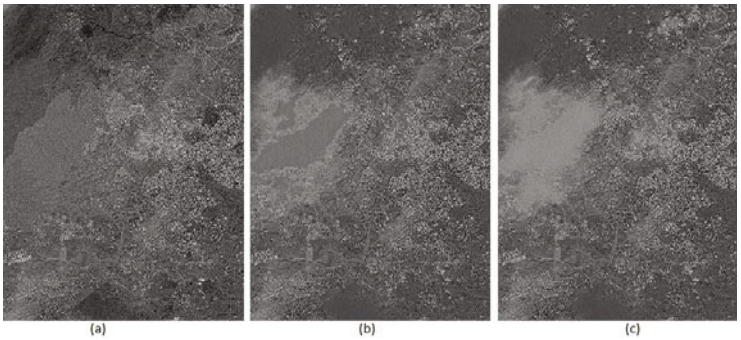

Fig. 5. Third test: (a) Reference image free of noise. The influence of *cn* and *cs* in clouds and shadows removal using HPF: (b) Butterworth ($Kappa = 0.5279$ and $PSNR = +19.64dB$) and (c) High boost ($Kappa = 0.5329$ and $PSNR = +19.94dB$)

Table 1. Evaluation of differents approaches in the proposed algorithm. The PSNR index is given in dB

Tested Images	Butterworth		High boost		Butterworth+constants		High boost+constants		Constants	
	Kappa	PSNR	Kappa	PSNR	Kappa	PSNR	Kappa	PSNR	cn	cs
Brasília	0.3940	18.54	0.5660	19.12	0.4626	18.41	0.6019	19.18	0.75	1.3
Belém 1	0.4471	24.44	0.7185	26.29	0.4572	24.57	0.7239	26.72	0.9	1.2
Fires	0.4669	21.33	0.4751	22.86	0.4858	24.49	0.5302	25.92	0.2	1
Alabama	0.5312	19.75	0.5368	20.23	0.6446	20.26	0.6702	21.16	1.5	1.1
Belém 2	0.6971	19.84	0.7035	20.61	0.7014	20.30	0.7492	20.94	0.9	1.2
Italy	0.6850	22.61	0.7131	23.04	0.7285	24.54	0.7295	24.76	0.5	1.25
Nasa	0.8217	26.78	0.8236	26.93	0.8351	26.26	0.8408	27.28	7	100
Ikonos 1	0.8312	24.23	0.8472	24.46	0.8445	24.43	0.8590	24.67	0.75	11
Lake	0.4982	12.86	0.5118	20.67	0.5452	13.82	0.6795	23.40	0.25	100
Ikonos 2	0.7814	24.79	0.7814	27.14	0.7862	26.65	0.7997	27.25	1.25	100
Andes	0.5292	17.89	0.5366	16.95	0.6025	18.58	0.6116	17.22	100	100
Capim	0.1803	17.19	0.6432	25.31	0.1867	17.42	0.6486	25.17	1.1	1.1
Macapá	0.2161	20.09	0.6487	26.13	0.7619	26.63	0.7501	27.36	0.8	1.5
Tucuruí	0.7583	21.91	0.8105	22.32	0.7991	24.31	0.8584	25.54	2.25	1.4
Belém 3	0.7378	22.66	0.8173	23.91	0.7710	23.04	0.8445	24.15	0.6	3

The method proposed was then applied to other 14 images. The Table 1 presents results in 15 different scenes (including the scene 'Italy' used to exemplify the method), where can be seen the superiority of the proposed method. It's important reinforce that such method, as well as others of the inpainting,

works well for small damaged regions, however, when the reconstruction area is too large, its results can produces blurred and unreal areas, without information of texture [11,2]. This effect was evidenced on a dense cloud region of the scene shown in that article.

4 Conclusion

In this paper, we deal with the removal of undesirable elements in the atmosphere such as fog, mist, clouds and the shadows from them, that damage and lead to loss of image data. Thus, we propose a method for removing such elements, which uses several techniques. Was highlighted in our method, a more efficient way to detect clouds and shadows with the aid of constants related to such elements, as well as the use of High-Boost Filter during the homomorphic filtering, comparing with the approaches applied in [7]. By results, aided by Kappa and PSNR index, we conclude that HPF High boost is more efficient than Butterworth, and that the use of the constants for region detection improve the final results of the algorithm, leading to the disappearance or smoothing of most noisy regions, as showed in the resultants figures, including the Fig. 6.

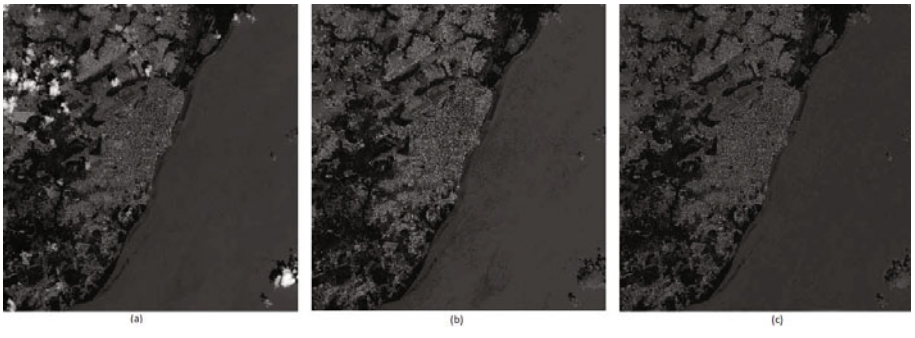

Fig. 6. Tested image 'Macapá': (a) Reference image free of noise. The influence of *cn* and *cs* in clouds and shadows removal using HPF: (b) Butterworth ($Kappa = 0.7619$ and $PSNR = +26.63dB$) and (c) High boost ($Kappa = 0.7501$ and $PSNR = +27.36dB$)

References

1. Bertalmio, M., Sapiro, G., Caselles, V., Ballester, C.: Image inpainting. In: Proceedings of the 27th Annual Conference on Computer Graphics and Interactive Techniques, pp. 417–424 (2000)
2. Criminisi, A., Pérez, P., Toyama, K.: Region filling and object removal by exemplar-based image Inpainting. IEEE Transactions On Image Processing 13, 1200–1212 (2004)
3. Delac, K., Grgic, M., Kos, T.: Sub-image Homomorphic filtering technique for improving facial identification under dificult illumination conditions. In: International Conference on Systems, Signals and Image Processing, pp. 95–98 (2006)

4. Delac, K., Mislav, G.: Handbook Of Data Compression. Springer, Heidelberg (2009)
5. Gonzalez, R.C., Woods, R.E.: Digital Image Processing. Addison-Wesley Publishing Company, Reading (2008)
6. Hale, D.: Image-guided blended neighbor interpolation of scattered data. In: 79th Annual International Meeting, Society of Exploration Geophysicists, vol. 28, pp. 1127–1131 (2009)
7. Hau, C.Y., Liu, C.H., Chou, T.Y., Yang, L.S.: The efficacy of semi-automatic classification result by using different cloud detection and diminution method. In: The International Archives of the Photogrammetry, Remote Sensing and Spatial Information Sciences (2008)
8. Hoan, N.T., Tateishi, R.: Cloud removal of optical image using SAR data for ALOS applications. Experimenting on simulated ALOS data. In: The International Archives of the Photogrammetry, Remote Sensing and Spatial Information Sciences (2008)
9. Htwe, A.N.: Image interpolation framework using non-adaptive approach and nl means. International Journal of Network and Mobile Technologies 1 (2010)
10. Kekre, H.B., Athawale, A., Halarnkar, P.N.: High payload using High Boost filtering in Kekre's Multiple LSB's algorithm. In: 2nd International Conference on Advances in Computer Vision and Information Technology (2009)
11. Kwok, T., Sheung, H., Wang, C.: Fast query for exemplar-based image completion. IP 19, 3106–3115 (2010)
12. Liu, H., Wang, W., Bi, X.: Study of image inpainting based on learning. In: Proceedings of The International MultiConference of Engineers and Computer Scientists, pp. 1442–1445 (2010)
13. Ma, J., Gu, X., Feng, C., Guo, J.: Study of thin cloud removal method for CBERS-02 image. Science in China Series E 48(2)(2005-03), 72–90 (2005)
14. Maalouf, A., Carre, P., Augereau, B., Fernandez Maloigne, C.: A bandelet-based Inpainting technique for clouds removal from remotely sensed images. IEEE Transactions On Geoscience And Remote Sensing 47(7), 2363–2371 (2009)
15. Salomon, D., Motta, G.: Handbook Of Data Compression. Springer, Heidelberg (2009)
16. Seow, M., Asari, V.: Ratio rule and homomorphic filter for enhancement of digital colour image. In: Proceedings of Neurocomputing, pp. 954–958 (2006)
17. Tasdizen, T., Whitaker, R., Burchard, P., Osher, S.: Geometric surface processing via normal maps. In: Proceedings of ACM Trans. Graph., pp. 1012–1033 (2003)
18. Zhang, X., Qin, F., Qin, Y.: Study on the thick cloud removal method based on multi-temporal remote sensing images. In: International Conference on Multimedia Technology (ICMT), pp. 1–3 (2010)